

Improvement of Spectral Editing in Solids: A Sequence for Obtaining $^{13}\text{CH} + ^{13}\text{CH}_2$ -Only ^{13}C Spectra

Sean T. Burns, Xiaoling Wu, and Kurt W. Zilm

Department of Chemistry, Yale University, 350 Edwards Street, New Haven, Connecticut 06511

Received August 12, 1999; revised December 7, 1999

An improved spectral editing method for solids is described which allows one to obtain a set of subspectra in roughly two-thirds the amount of time as our original CPPI editing method for the same signal to noise. This improvement is afforded by a new pulse sequence that is used to acquire a $^{13}\text{CH} + ^{13}\text{CH}_2$ spectrum which has very little $^{13}\text{CH}_3$ or nonprotonated carbon contamination. By using this new sequence the ^{13}CH -only subspectrum is obtained much more efficiently. Criteria for optimizing the signal to noise in the edited subspectra are discussed. © 2000 Academic Press

Key Words: solid-state; spectral editing; CPMAS; signal-to-noise ratio (S/N); CP dynamics.

INTRODUCTION

The combination of cross polarization (CP) with magic angle spinning (MAS) and high power proton decoupling constitutes one of the most popular solid-state NMR experiments. Routine application of this experiment in laboratories around the world results in high-resolution, liquid-like spectra of a wide range of organic solids. Spectral editing is an important assignment tool for such spectra, especially in industrial applications to hydrocarbon mixtures and polymers. In solution state NMR, spectral editing is well developed (1), and numerous approaches to editing exist. Solution NMR editing methods rely on evolution of ^{13}C magnetization under scalar couplings and the fact that $^1J_{\text{CH}}$ falls in a characteristic and narrow range of values. Since these couplings are not typically resolvable in the solid state, editing methods for solids NMR are more often based on evolution under dipolar couplings.

We have recently proposed methods that rely upon the domination of CP dynamics at short times by the strong dipolar couplings between a ^{13}C nucleus and its directly bonded protons, and the ratio of the heat capacities of the ^{13}C and these directly attached protons. Methods of this type are less sensitive to molecular mobility than those which rely only on the strength of the ^{13}C - ^1H dipolar interactions. The relative merits of such an approach in comparison to many other methods (2–11) used to edit complex ^{13}C spectra of solids have been discussed elsewhere (12).

In our most recent method (cross polarization-polarization inversion or CPPI editing) (12) four spectra are combined to

obtain the nonprotonated ^{13}C (hereafter abbreviated as ^{-13}C), ^{13}CH , $^{13}\text{CH}_2$, and $^{13}\text{CH}_3$ subspectra. A sequence consisting of a short contact time cross polarization (SCP) followed by a short polarization inversion (PI) interval (SCPPI) is used to obtain the $^{13}\text{CH}_2$ -only subspectrum. To obtain a ^{13}CH -only subspectrum three spectra are combined. Using a SCP sequence, a spectrum dominated by ^{13}CH and $^{13}\text{CH}_2$ signals is obtained. Subtraction of the SCPPI spectrum results in a ^{13}CH -dominated spectrum. Unfortunately the intensity of the ^{-13}C - and $^{13}\text{CH}_3$ signals in this difference spectrum is too large for this alone to be a useful means of producing ^{13}CH -only subspectra. These undesired signals are, however, closely reproduced in a spectrum acquired using a SCP sequence that is followed by a depolarization interval (SCPD) which cleanly removes the ^{13}CH and $^{13}\text{CH}_2$ resonances. A second subtraction can then be used to generate a good ^{13}CH -only subspectrum, albeit at a heavy penalty in signal-to-noise ratio (S/N). (12). Methyl and nonprotonated subspectra are obtained from the LCPD (long CP – depolarization) spectrum. Separation of these two carbon types relies upon the fact that the chemical shift ranges most often do not overlap. In many applications this is justified; however, it is an inherent weakness of the general approach we have developed.

This paper describes the use of a sequence we call cross polarization dipolar dephasing re-cross polarization (CPD-DRCP). This sequence is used to obtain a $^{13}\text{CH} + ^{13}\text{CH}_2$ -only spectrum in which the ^{-13}C - and $^{13}\text{CH}_3$ resonances are more completely suppressed. This makes generation of the ^{13}CH -only subspectrum feasible with a single subtraction and reduces the amount of time needed to collect a spectral editing data set considerably. The remaining subspectra which take less time to acquire are obtained in the same way as before. While the CPPI editing protocol is still found to produce the most accurately edited data in terms of quantitation, the new method does produce results that are of comparable quality and is preferable if signal to noise is at a premium.

THE CP-DIPOLAR-DEPHASING-RE-CP SEQUENCE

The sequence shown in Fig. 1a has been devised with the aim of producing a $^{13}\text{CH} + ^{13}\text{CH}_2$ -only spectrum. In the first

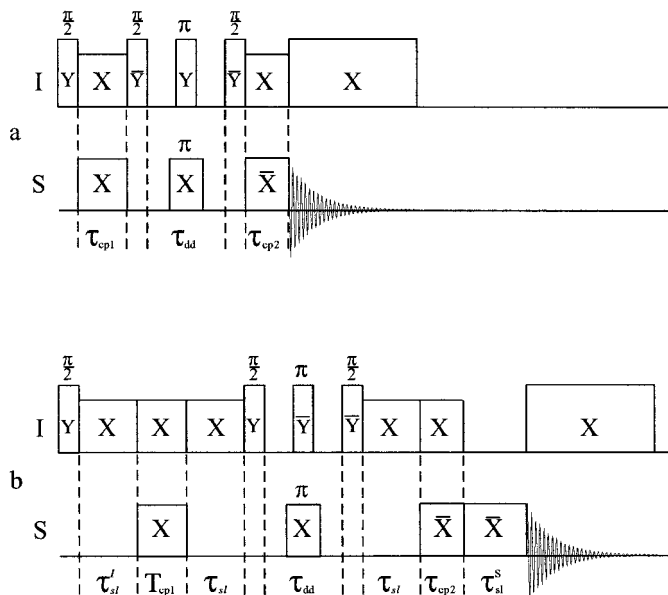


FIG. 1. The CPDDRCP sequence used to acquire $^{13}\text{CH} + ^{13}\text{CH}_2$ -dominated spectra. (a) Simplified sequence illustrating the basic idea. (b) Sequence as used showing the optional rotor synchronization. The timing is as follows: $\tau_{sl}^I = 140 \mu\text{s}$; $\tau_{cp1} = 56 \mu\text{s}$; $\tau_{dd} = 50 \mu\text{s}$; $\tau_{cp2} = 40 \mu\text{s}$; $\tau_{sl}^S = 400 \mu\text{s}$; τ_{sl} is determined based on the spinning speed.

step a short cross polarization is applied which polarizes the ^{13}CH and $^{13}\text{CH}_2$ groups to a quasi-equilibrium state. A small amount of ^{-13}C - and $^{13}\text{CH}_3$ polarization is also produced. At this point the ^1H magnetization has been largely unaffected; application of a $\pi/2$ pulse with a $\pi/2$ phase shift in the ^1H channel returns the ^1H magnetization to the z axis where it can be stored. The ^{13}C magnetization is then permitted to evolve with no ^1H RF applied, causing the ^{13}CH and $^{13}\text{CH}_2$ signals to dephase during the interval τ_{dd} . Refocusing of the chemical shift evolution during this interval places the small ^{-13}C - and $^{13}\text{CH}_3$ magnetizations back in phase where they can be spinlocked once more. This spinlocked state becomes the starting point for a second SCP period. By proper adjustment of the relative phases, the ^{-13}C - and $^{13}\text{CH}_3$ signals are now depolarized, whereas the ^{13}CH and $^{13}\text{CH}_2$ groups, which are starting with no net polarization, are allowed to again reach their quasi-equilibrium intensities. The resulting spectrum will contain ^{13}CH and $^{13}\text{CH}_2$ signals with intensities similar to those obtained in a SCP experiment. The principal difference is that the ^{-13}C - and $^{13}\text{CH}_3$ error signals are now greatly reduced in intensity. The intensity and sign of these error signals depend on the relative length of the two CP periods.

The timing of the pulse sequence was determined as follows. The second CP period, τ_{cp2} , was chosen to be $40 \mu\text{s}$ to bring the CH and CH_2 carbons to their quasi-equilibrium state. The dipolar dephasing time ($\tau_{dd} = 50 \mu\text{s}$) was the minimum time needed to null the CH and CH_2 signals. It was not possible to completely eliminate the ^{-13}C - and $^{13}\text{CH}_3$ signals simultaneously under these conditions. Therefore, once τ_{cp2} and τ_{dd}

were determined, the initial CP time, τ_{cp1} , was arrayed to find the null points for either the ^{-13}C - or the CH_3 resonances.

A number of variations are possible on this basic scheme. The dephasing interval can be done in a rotor synchronized fashion to eliminate dephasing from chemical shift anisotropy (CSA) effects. This can be especially important at higher fields. On the other hand this does introduce signal loss from T_2 during the dipolar dephasing delay. At low fields and moderate spin rates one may find asynchronous operation more efficient. Other methods for dephasing the ^{13}CH and $^{13}\text{CH}_2$ signals are also possible in theory. However, we have found that depolarization and other multiple-pulse schemes for dephasing the ^{13}C signals also result in substantial, often total, loss of ^1H magnetization. Since the basic method described here relies on having essentially the full ^1H magnetization available for the final SCP step, these alternatives are at the moment impractical.

Figure 1b shows the CPDDRCP sequence as it is used in practice. A short initial proton spinlock (τ_{sl}^I) of $140 \mu\text{s}$ is added to allow both the proton amplifier and the spin temperature to stabilize. The dephasing period may be bracketed by proton spinlocks (τ_{sl}) chosen to rotor synchronize the π pulses. Finally, a carbon spinlock is added to the end of the sequence to minimize differential $T_{1\rho}$ effects among the editing sequences.

As mentioned, the length of the initial CP can be varied to modulate the sign and magnitude of the ^{-13}C - and $^{13}\text{CH}_3$ error signals. A $56\text{-}\mu\text{s}$ initial CP will yield a spectrum with slightly positive methyl signal and near zero nonprotonated signal. If the initial CP is longer, the nonprotonated resonances will be slightly negative and the methyls will be near zero. An intermediate timing can be chosen such that the nonprotonated and methyl resonances are both near zero. This intermediate-timed spectrum will have ^{-13}C - and $^{13}\text{CH}_3$ error signals with magnitudes less than 0.05 relative to the LCP spectrum. In some cases, a ^{13}CH -only subspectrum can be obtained directly from this spectrum by simply subtracting out the $^{13}\text{CH}_2$ signal. For comparison to the original CPPI editing method, a $56\text{-}\mu\text{s}$ initial CP was chosen. This yields a spectrum with relative methyl intensities of 0.07 which can be easily subtracted at a small decrease in S/N . Figure 2 shows a comparison of this CPDDRCP spectrum (Fig. 2b) and the SCP spectrum (Fig 2a). From

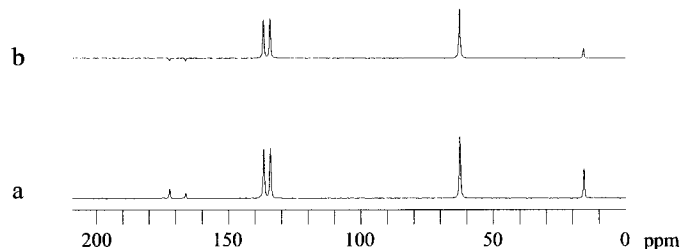


FIG. 2. Monoethyl fumarate spectra. (a) SCP and (b) CPDDRCP spectra.

TABLE 1
Matrix of Spectral Intensities s_{ij}

Carbon type:	j	$-^{13}\text{C}-$	^{13}CH	$^{13}\text{CH}_2$	$^{13}\text{CH}_3$
		0	1	2	3
Experiment	i				
LCP	0	1.00	1.00	1.00	1.00
CPDDRCP	1	0	0.42	0.57	0.07
SCPPI	2	0	0	-0.24	0
LCPD	3	0.86	0	0	0.61
SCP	4	0.09	0.57	0.69	0.24
SCPD	5	0.08	0	0	0.12

this figure it can be seen that the $-^{13}\text{C}-$ and $^{13}\text{CH}_3$ signals are suppressed better with the new sequence.

Similar to the earlier method (12), the editing protocol requires the experimenter to take spectra of a model compound using the editing pulse sequences to calibrate their particular instrument and to empirically account for departures from the idealized spectral intensities predicted from the quasi-equilibrium theory. These discrepancies are a result of long-range CP transfer and from $^1\text{H}/^1\text{H}$ spin diffusion as we have discussed before. As such, calibration on a known model compound with similar ^1H density goes a long way toward accounting for such effects in an unknown sample where the H/C ratio can be obtained from elemental analysis. These intensity matrix values were calibrated for the currently used experimental setup and as expected are slightly different from those published previously (12). The resulting intensity matrix defines the linear combinations used to generate subspectra for a given carbon type. In each column the matrix elements give the intensity of the indicated carbon type for the experiment specified by the row label (see Table 1).

A matrix element s_{ij} represents the intensity of the j th resonance in the i th experiment measured relative to the cor-

responding (i.e., the j th) resonance in the LCP spectrum for the same number of scans. In Table 1 we have included spectra from the CPPI method as well as the CPDDRCP method.

The intensity matrix is used as a guide to form the subspectra. In general the j th subspectrum $S_j(\omega)$ is formed by taking a linear combination of the i experimental spectra $E_i(\omega)$ as

$$S_j(\omega) = \sum_i \frac{a_{ij}E_i(\omega)}{A_i} = \sum_i a_{ij}\epsilon_i(\omega). \quad [1]$$

Equation [1] defines the linear expansion coefficients, a_{ij} , and the $\epsilon_i(\omega)$, which are the experimental spectra scaled by the relative number of scans, A_i . The linear expansion coefficients are calculated from the intensity matrix elements, s_{ij} , and are listed in Table 2. Each subspectrum is represented by a column in the table. The rows represent the experimental spectra. The table entries are then the a_{ij} 's which are the coefficients the scaled experimental spectra must be multiplied by to form the subspectra. The subscript i is used to denote the pulse sequence used and j indexes the proton multiplicity of the resonances in the spectra.

As can be seen from Table 2, some of these combinations are quite simple. The $^{13}\text{CH}_2$ -only subspectrum, $S_2(\omega)$, is formed from the experimental SCPPI spectrum, $E_2(\omega)$, scaled by the number of scans, A_2 , as $S_2(\omega) = (1/s_{22})E_2(\omega)/A_2 = 1/s_{22}\epsilon_2(\omega)$. The $^{13}\text{CH}_3$ -only subspectrum is formed from the scaled LCPD spectrum, $\epsilon_3(\omega)$, by multiplying it by $1/s_{33} = 1/0.61$ and removing the region containing $-^{13}\text{C}-$ signal. The $-^{13}\text{C}-$ only subspectrum is formed from the scaled LCPD spectrum by multiplying it by $1/s_{30} = 1/0.86$ and then zeroing the $^{13}\text{CH}_3$ region. Only the ^{13}CH subspectrum requires a linear combination of several spectra to be made. To form $S_1(\omega)$, one starts with the CPDDRCP spectrum and subtracts the $^{13}\text{CH}_2$ and $^{13}\text{CH}_3$ contributions. From Table 2 one finds $S_1(\omega) =$

TABLE 2
Linear Coefficients, a_{ij} , Used to Form the Subspectra

i	$S_0(\omega)$	$S_j(\omega)$ CPDDRCP method			$S_j(\omega)$ CPPI method				
		$S_1(\omega)$	$S_2(\omega)$	$S_3(\omega)$	$S_0(\omega)$	$S_1(\omega)$	$S_2(\omega)$	$S_3(\omega)$	
CPDDRCP	1	0	$\frac{1}{s_{11}}$	0	0	—	—	—	—
SCPPI	2	0	$\frac{-s_{12}}{s_{22}s_{11}}$	$\frac{1}{s_{22}}$	0	0	$\frac{-s_{42}}{s_{22}s_{41}}$	$\frac{1}{s_{22}}$	0
LCPD	3	$\frac{1}{s_{30}}$	$\frac{-s_{13}}{s_{33}s_{11}}$	0	$\frac{1}{s_{33}}$	$\frac{1}{s_{30}}$	0	0	$\frac{1}{s_{33}}$
SCP	4	—	—	—	—	0	$\frac{1}{s_{41}}$	0	0
SCPD	5	—	—	—	—	0	$\frac{-s_{43}}{s_{33}s_{41}}$	0	0

$$[a_{11}\epsilon_1(\omega) + a_{21}\epsilon_2(\omega) + a_{31}\epsilon_3(\omega)] = [(1/s_{11})\epsilon_1(\omega) + (-s_{12}/(s_{22}s_{11}))\epsilon_2(\omega) + (-s_{13}/(s_{33}s_{11}))\epsilon_3(\omega)].$$

SIGNAL TO NOISE CONSIDERATIONS

Typically the application of these spectral editing methods will result in a set of subspectra for a given compound. These subspectra may be analyzed quantitatively to determine relative (or possibly absolute) amounts of the different carbon types. When doing this type of analysis, there is no advantage to having greater S/N in one subspectrum or another. It would therefore seem appropriate to have roughly equal signal to noise in each of the subspectra. It is straightforward to calculate the correct numbers of scans to give similar S/N for the ^{13}C -, $^{13}\text{CH}_2$, and $^{13}\text{CH}_3$ subspectra, as these subspectra are formed from a single spectrum each. For example, in order for the $^{13}\text{CH}_2$ -only subspectrum to have the same S/N as the LCP spectrum one must acquire $(1/0.24)^2$ or 17.4 times more scans. However, it is not immediately obvious, given a set of values for the experimental numbers of scans, what the ^{13}CH -only S/N will be and whether the ^{13}CH -only S/N is the optimum for the amount of time used. The situation for the ^{13}CH -only subspectrum is more complicated than the others since it is formed from a linear combination of the CPDDRCP (or SCP), LCPD (or SCPD), and SCPPI spectra. To aid in finding the correct numbers of scans to acquire, the S/N of the ^{13}CH -only subspectrum expressed in terms of the intensity matrix elements and the numbers of scans will be examined. Such an expression can be written for a ^{13}CH -only subspectrum derived from either the CPPI or the CPDDRCP protocol and can be used to determine the advantage of one method over the other. In general, the S/N of the j th subspectrum is written

$$\left(\frac{S}{N}\right)_j = \frac{\sum_i a_{ij}s_{ij}}{\left(\sum_i \frac{n_i^2 a_{ij}^2}{A_i}\right)^{1/2}}, \quad [2]$$

where n_i is the noise in one scan.

First let us consider the CPDDRCP method. Substituting the appropriate a_{ij} 's from Table 2 into Eq. [2] yields Eq. [3], which gives the S/N for the ^{13}CH -only subspectrum,

$$\left(\frac{S}{N}\right)_1 = \frac{s_{11}}{n_1} \left(\frac{1}{A_1} + \frac{(s_{12}/s_{22})^2}{A_2} + \frac{(s_{13}/s_{33})^2}{A_3} \right)^{-1/2}, \quad [3]$$

where $s_{21} = s_{31} = 0$ has been used.

The goal is then to maximize this expression but we need to determine the appropriate constraints. The equal S/N criterion mentioned earlier can be most nearly accommodated by constraining the S/N for the ^{13}CH -only subspectrum to be equal to the S/N for the $^{13}\text{CH}_3$ -only subspectrum. This constraint ensures that the S/N of the individual subspectra are roughly equal and that undue time is not spent improving the S/N of

one subspectrum at the expense of the others. The second constraint is that the total time must be fixed ($A_1 + A_2 + A_3 = \text{constant}$). Equation [3] was maximized using Lagrange's method of undetermined multipliers subject to these constraints. One obtains

$$A_2 = |s_{12}/s_{22}|A_1; \quad A_3 = A_1 \left(\frac{(s_{11}/s_{33})^2 - (s_{13}/s_{33})^2}{1 + |s_{12}/s_{22}|} \right) \quad [4]$$

for the optimum numbers of scans for the individual experimental spectra. Using these numbers of scans, one finds that the S/N for the ^{13}CH -only and the $^{13}\text{CH}_3$ -only subspectra are equal while the S/N for the $^{13}\text{CH}_2$ and ^{13}C -only subspectra are somewhat better.

The numbers of scans for the CPPI method can be similarly optimized. Here, we will use B_i instead of A_i to denote the numbers of scans. The S/N for the ^{13}CH -only subspectrum obtained by the CPPI method is given by

$$\left(\frac{S}{N}\right)_1 = \frac{s_{41}}{n_1} \left(\frac{1}{B_4} + \frac{(s_{42}/s_{22})^2}{B_2} + \frac{(s_{43}/s_{53})^2}{B_5} \right)^{-1/2}, \quad [5]$$

where $s_{21} = s_{51} = 0$ has been used. The optimum numbers of scans are found to be

$$B_2 = |s_{42}/s_{22}|B_4; \quad B_5 = (s_{43}/s_{53})B_4; \\ B_3 = B_4 \left(\frac{(s_{41}/s_{33})^2}{1 + |s_{42}/s_{22}| + (s_{43}/s_{53})} \right). \quad [6]$$

In the CPPI method, experiment 4 is the SCP and experiment 5 the SCPD. Experiments 2 and 3 are still the SCPPI and LCPD, respectively.

The advantage in terms of time saved by using the CPDDRCP method over the CPPI method can be calculated as the ratio of the total experimental time in the two cases when the ^{13}CH -only subspectrum has the same S/N ratio. Setting $A_3 = B_3$ one obtains

$$\frac{A_1 + A_2 + A_3}{B_2 + B_3 + B_4 + B_5} = 0.63, \quad [7]$$

which means that the CPDDRCP method will require less than two-thirds of the time to obtain the same S/N as the CPPI method.

Using these relationships a table illustrating the recommended numbers of scans for each experiment in the two protocols can be produced (Table 3).

EXPERIMENTAL

All experiments were performed on a homebuilt NMR spectrometer based on a Tecmag Libra data system and

TABLE 3
Optimum Numbers of Scans for the Individual Experiments
in Each Editing Protocol

Experiment	CPDDRCP	CPPI
CPDDRCP	7.3A ₃	—
SCPPI	17.4A ₃	19.3A ₃
LCPD	A ₃	A ₃
SCP	—	6.7A ₃
SCPD	—	13.5A ₃
Total	25.7A ₃	40.5A ₃

using an Oxford Instruments 2.35-T, 110-mm room-temperature bore superconducting solenoid. A homebuilt CPMAS probe incorporating a 7-mm MAS stator with a variable pitch RF coil from Doty Scientific was used. Samples were spun at the magic angle at 4.0 kHz. The spin rate was determined using a triboelectric tachometer and observed to vary no more than ± 20 Hz over a 24-h period. Spin rate regulation is accomplished solely by regulating the air supply with two successive two-stage regulators. The magic angle was set by minimizing the aromatic centerband linewidth for a sample of hexamethylbenzene as the angle was varied. Typically 19 Hz is the minimum linewidth obtained under these conditions. For monoethyl fumarate proton decoupling was accomplished at 3.0 ppm with a 95-kHz decoupling field. Cholesteryl acetate spectra were acquired with a decoupling amplitude of 95 kHz for the first 250 ms and 60 kHz for the remaining 258 ms of the acquisition. The Hartmann–Hahn match condition was set at $\gamma_I H_1^I = \gamma_S H_1^S = 55$ kHz by maximizing the adamantane signal as a function of ^{13}C RF field strength. For this determination, a sample of adamantane was spun at ca. 800 Hz in order to remove the possibility of accidentally finding a sideband match. A CP time of 500 μs was used while the match was being set. Once the best match was found, SCPPI and LCPD experiments using a sample of monoethyl fumarate were performed. Absence of ^{-13}C -, ^{13}CH -, and $^{13}\text{CH}_3$ signal in the SCPPI spectrum and absence of ^{13}CH and $^{13}\text{CH}_2$ signal in the LCPD spectrum confirms that the match is well set.

Editing data for monoethyl fumarate and cholesteryl acetate were obtained on samples purchased from Aldrich. Edited subspectra were generated by linear combinations of the experimental data according to the intensity matrix obtained for a single model compound (monoethyl fumarate). The results were evaluated by comparing the “synthetic” LCP spectrum constructed by summing the individual subspectra to an experimentally obtained LCP spectrum. Discrepancies in the intensities of the resonances obtained in these two spectra, as seen in their difference spectrum, were taken as indicative of the size of the errors inherent in the method.

RESULTS

Spectra of monoethyl fumarate (Fig. 3) and cholesteryl acetate (Fig. 4) were acquired in order to test the new pulse sequence. The normal CPMAS spectrum of monoethyl fumarate consists of six lines (Fig. 3a). There are two ^{-13}C -resonances near 166 and 172 ppm, two ^{13}CH resonances near 135 ppm, a $^{13}\text{CH}_2$ resonance at 62.7 ppm, and a $^{13}\text{CH}_3$ resonance at 15.9 ppm. In the $^{13}\text{CH} + ^{13}\text{CH}_2$ -dominated CPDDRCP spectrum (Fig. 3b), the ^{-13}C -signals are essentially absent and the $^{13}\text{CH}_3$ signal is small with an intensity of 0.07 relative to its LCP value. The ^{13}CH and $^{13}\text{CH}_2$ relative signal intensities lie near their quasi-equilibrium values at 0.42 and 0.57, respectively. The SCPPI spectrum (Fig. 3c) contains a single negative peak corresponding to the $^{13}\text{CH}_2$ group and a pair of extremely small positive ^{-13}C -error signals. The ^{13}CH signal is well suppressed as predicted by the quasi-equilibrium theory and the $^{13}\text{CH}_3$ intensity is zero. The relative intensity of this $^{13}\text{CH}_2$ resonance is -0.24 . The final spectrum required in order to complete the editing protocol is the LCPD spectrum (Fig. 3d). In this depolarization spectrum the ^{-13}C -resonances are attenuated to 0.86 relative to the LCP. $^{13}\text{CH}_3$ resonances are also attenuated, with a relative intensity of 0.61. These intensities are tabulated in the intensity matrix (Table 1). In the LCPD spectrum, depolarization has reduced the ^{13}CH and $^{13}\text{CH}_2$ resonances to a relative intensity of <0.01 . A spinning sideband from one of the ^{-13}C -resonances is visible just to the right of the methyl peak at 9.9 ppm. There is another under the right edge of the methyl peak.

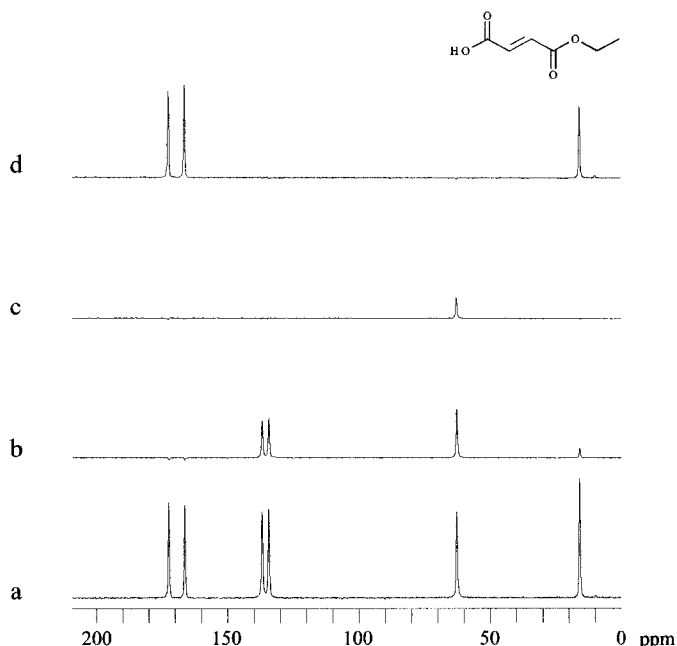


FIG. 3. Monoethyl fumarate spectra. (a) LCP; (b) $^{13}\text{CH} + ^{13}\text{CH}_2$ -dominated; (c) SCPPI; (d) LCPD. The SCPPI spectrum is plotted upside down for ease of display.

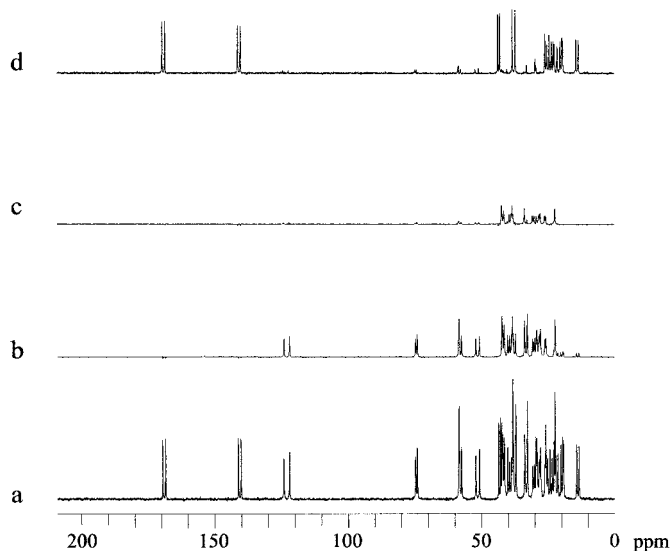
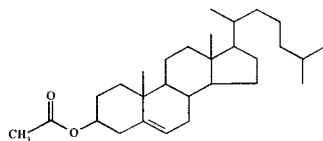


FIG. 4. Cholesteryl acetate spectra. (a) LCP; (b) $^{13}\text{CH} + ^{13}\text{CH}_2$ -dominated; (c) SCPPI; (d) LCPD. The SCPPI spectrum is plotted upside down for ease of display.

Since cholesteryl acetate has 29 carbon centers and there are two distinct molecules in each unit cell one would expect to observe 58 separate resonances for this compound; however, at this field strength they are not all resolved (see Fig. 4). LCP spectra (Fig. 4a) of this compound show complex spectra with several overlapping resonances. The $^{13}\text{CH} + ^{13}\text{CH}_2$ -dominated spectrum (Fig. 4b) clearly shows that the $^{-13}\text{C}-$ signals are suppressed. The two downfield doublets arising from a carbonyl and the nonprotonated alkene carbon are both reduced to less than 0.03 in this $^{13}\text{CH} + ^{13}\text{CH}_2$ -dominated spectrum. The SCPPI spectrum (Fig. 4c) shows the $^{13}\text{CH}_2$ resonances clearly. Several small signals can also be seen that are due to imperfectly nulled ^{13}CH resonances. The $^{-13}\text{C}-$ resonances show up as very small negative error signals. In the LCPD spectrum (Fig. 4d), the ^{13}CH and $^{13}\text{CH}_2$ resonances are suppressed except for several small positive ^{13}CH signals. The $^{-13}\text{C}-$ and $^{13}\text{CH}_3$ resonances can be clearly seen.

Edited subspectra of monoethyl fumarate are displayed in Fig. 5. In the $^{-13}\text{C}-$ subspectrum (Fig. 5a), the ^{13}CH and $^{13}\text{CH}_2$ peaks are well nulled. The region from 0 to 27 ppm has been zeroed to remove the methyl signal. The ^{13}CH subspectrum (Fig. 5b) has two small out of phase signals from $^{-13}\text{C}-$ carbons but otherwise looks very clean. The $^{13}\text{CH}_2$ -only subspectrum (Fig. 5c) is contaminated with very small negative $^{-13}\text{C}-$ signals. The methyl-only subspectrum (Fig. 5d) contains spinning sidebands from the $^{-13}\text{C}-$ resonances. One is under the right edge of the methyl peak and the other is visible beside the

peak. The region from 27 to 209 ppm has been zeroed to remove $^{-13}\text{C}-$ signal. Figure 5e is the LCP spectrum from Fig. 3a redisplayed for comparison with Fig. 5f, which is the synthetic LCP spectrum obtained by summing the subspectra (Figs. 5a–5d). The difference spectrum (Fig. 5g) is the result of subtraction of the synthetic LCP spectrum from the normal LCP spectrum. The difference is very good except for some small negative nonprotonated error signals.

Edited subspectra were also obtained for cholesteryl acetate (Fig. 6) using the intensity matrix measured for monoethyl fumarate. The $^{-13}\text{C}-$ only subspectrum (Fig. 6a) is quite clean with the only errors being the small, incompletely depolarized ^{13}CH signals. The region from 0 to 27 ppm has been zeroed to remove $^{13}\text{CH}_3$ signals. The largest of the error signals in the ^{13}CH -only subspectrum (Fig. 6b) is due to a $^{13}\text{CH}_2$ resonance near 42 ppm. Other error peaks, also traceable to $^{13}\text{CH}_2$ resonances, are negative and of smaller intensity. Two nonprotonated resonances, overlapped by the methylene envelope in the $^{13}\text{CH} + ^{13}\text{CH}_2$ spectrum, show small error peaks in this subspectrum. The $^{13}\text{CH}_2$ -only subspectrum (Fig. 6c) has small error peaks for most of the ^{13}CH resonances, the largest of which comes at 60 ppm. The $^{13}\text{CH}_3$ -only subspectrum (Fig. 6d) again has the region from 27 to 209 ppm zeroed to remove $^{-13}\text{C}-$ signal. Figure 6e is the LCP spectrum from Fig. 4a redisplayed for comparison with Fig. 6f, which is the synthetic

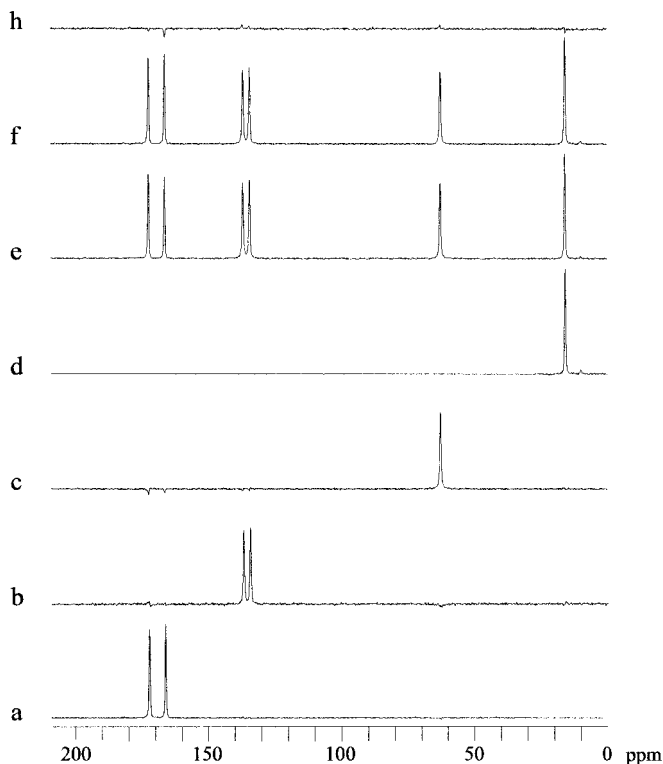


FIG. 5. Edited monoethyl fumarate subspectra. (a) $^{-13}\text{C}-$ only; (b) ^{13}CH -only; (c) $^{13}\text{CH}_2$ -only; (d) $^{13}\text{CH}_3$ -only; (e) LCP; (f) synthetic; (g) difference (e–f).

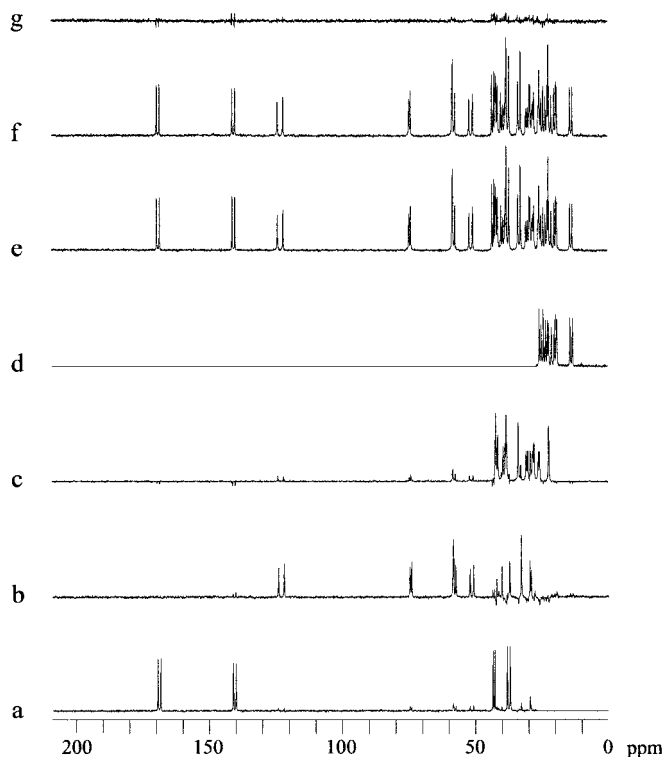


FIG. 6. Edited cholesteryl acetate subspectra. (a) ^{-13}C -only; (b) ^{13}CH -only; (c) $^{13}\text{CH}_2$ -only; (d) $^{13}\text{CH}_3$ -only; (e) LCP; (f) synthetic; (g) difference (e-f).

LCP spectrum obtained by summing the subspectra (Figs. 6a–6d). The difference spectrum (Fig. 6g) is essentially noise except for a few small peaks in the 20- to 40-ppm range and small out of phase nonprotonated signals that integrate to zero.

DISCUSSION

We have considered the S/N in the ^{13}CH -only subspectrum to determine the optimum numbers of scans for each of the editing experiments. This analysis confirms that the CPD-DRCP sequence provides edited subspectra with the same S/N as the CPPI method but only requires two-thirds the amount of time.

With the above optimization condition, the relative signal to noise ratios for the individual subspectra are $S_0(\omega):S_1(\omega):S_2(\omega):S_3(\omega) = 1.4:1:1.6:1$ in both the CPDDRC and the CPPI protocols. As mentioned before, $S_0(\omega)$ and $S_2(\omega)$ will always have better S/N . This is not accidental. Since the ^{13}C and $^{13}\text{CH}_3$ subspectra are both obtained from the same LCPD spectrum and the $^{13}\text{CH}_3$ resonances are attenuated more due to their stronger dipolar couplings, the S/N of $S_3(\omega)$ must be less than that of $S_0(\omega)$. For the $^{13}\text{CH}:^{13}\text{CH}_2$ case, it can be seen that the $^{13}\text{CH}_2$ will have better S/N due to the way the CPDDRC and SCPPI spectra are combined to form $S_1(\omega)$. Addition of the SCPPI spectrum to the CPDDRC spectrum with $a_{ij} > 1$

combined with the fact that the ^{13}CH intensity is less than the $^{13}\text{CH}_2$ intensity ensures that the sum spectrum will have worse S/N than the SCPPI. It was on the basis of this reasoning that we chose to constrain the S/N of the ^{13}CH to be equal to the S/N of the $^{13}\text{CH}_3$.

The CPPI editing method is useful for separating resonances in spectra of unknown compounds and complex mixtures into subspectra on the basis on the number of attached protons. Of the subspectra resulting from application of this method, the ^{13}CH -only subspectrum is clearly the most time consuming to obtain. With the method proposed here, reliance on the SCPD spectrum is removed and the ^{13}CH -only subspectrum can be obtained more quickly. Because of this advantage, the method will find application when signal to noise is poor. The CPD-DRCP sequence is, however, slightly more complicated experimentally than the original pulse sequences which kept the carbon magnetization spinlocked.

The monoethyl fumarate and cholesteryl acetate spectra obtained with these pulse sequences are very similar in quality to those obtained with the CPPI editing method. With either of these methods, small ^{13}CH error signals may sometimes be seen in the LCPD or the SCPPI spectra but these are usually less than a few percent. The $^{13}\text{CH} + ^{13}\text{CH}_2$ -dominated spectrum successfully reduces the time required to obtain the ^{13}CH -only subspectrum. Essentially, the editing method is applied in the same way as it was before; a depolarization spectrum is acquired and used as a source of ^{-13}C - and $^{13}\text{CH}_3$ signal. The $^{13}\text{CH}_2$ -only subspectrum is still obtained directly from the SCPPI spectrum and the ^{13}CH -only subspectrum is obtained from a spectrum similar to the SCP only without the ^{-13}C -signal (the $^{13}\text{CH} + ^{13}\text{CH}_2$ -dominated spectrum). With this new method it is no longer necessary to acquire the SCPD spectrum that was used to remove the ^{-13}C - and $^{13}\text{CH}_3$ signal from the SCP spectrum. This is the true advantage since the SCPD spectrum always had the worst signal-to-noise ratio of any spectrum in the set used for CPPI editing.

In our analysis, we have implicitly assumed that each resonance of the LCP spectrum is equally intense. This represents an ideal situation which will only be realized in practice when the spectra are well resolved and the widths of the resonances are equal. More generally, one can expect some deviation from the calculated S/N ratios due to differences in these and other parameters.

CONCLUSIONS

We have reported here a new pulse sequence that can be used to acquire a $^{13}\text{CH} + ^{13}\text{CH}_2$ -dominated spectrum. This spectrum is useful as part of an editing protocol in that it allows the ^{13}CH -only subspectrum to be obtained more directly. The $^{13}\text{CH} + ^{13}\text{CH}_2$ -dominated spectrum allows for the acquisition of a ^{13}CH -only subspectrum of equal or better quality to that obtained with the original method with the same signal-to-noise ratio in considerably less time. With the addition of the

$^{13}\text{CH} + ^{13}\text{CH}_2$ -dominated spectrum, the editing routine remains simple to set up.

These pulse sequences are of course not limited to editing applications solely for the purpose of spectral decomposition. Preparatory schemes based on these sequences can be implemented to prepare specific spin polarizations for more elaborate polarization transfer experiments.

The principal limitation of this method and our previous technique is the need to spin fast enough to suppress all CSA spinning sidebands, yet slow enough as not to severely disturb the cross polarization dynamics relied upon. Modifications of the protocols presented are being developed which will be better suited to high-field operation where much faster spin rates are desirable.

ACKNOWLEDGMENTS

Support of this work by EXXON Research and Engineering Corporation and the U.S. Department of Energy under Grant DE-F922-95PC95227 is gratefully acknowledged.

REFERENCES

1. R. R. Ernst, G. Bodenhausen, and A. Wokaun, "Principles of Nuclear Magnetic Resonance in One and Two Dimensions," The International Series of Monographs on Chemistry, pp. 192–201, Oxford Univ. Press, New York, 1987.
2. T. Terao, H. Miura, and A. Saika, Simplification and assignment of carbon-13 spectra by using J -resolved NMR spectroscopy in solids, *J. Am. Chem. Soc.* **104**, 5228–5229 (1982).
3. K. W. Zilm and D. M. Grant, High-resolution NMR spectra with J couplings in solids, *J. Magn. Reson.* **48**, 524–526 (1982).
4. M. Alla and E. Lippmaa, High resolution broad line ^{13}C NMR and relaxation in solid norbornadiene, *Chem. Phys. Lett.* **37**, 260–264 (1976).
5. S. J. Opella and M. H. Frey, Selection of nonprotonated carbon resonances in solid-state nuclear magnetic resonance, *J. Am. Chem. Soc.* **101**, 5854–5856 (1979).
6. J. Peng and L. Frydman, Spectral editing in solid-state MAS NMR using chemical-shift-anisotropy-dephasing techniques, *J. Magn. Reson. A* **113**, 247–250 (1995).
7. R. Sangill, N. Rastrup-Andersen, H. Bildsøe, H. J. Jakobsen, and N. C. Nielsen, Optimized spectral editing of ^{13}C MAS NMR spectra of rigid solids using cross-polarization methods, *J. Magn. Reson. A* **107**, 67–78 (1994).
8. D. P. Burum and A. Bielecki, WIMSE, a new spectral editing technique for CPMAS solid-state NMR, *J. Magn. Reson.* **95**, 184–190 (1991).
9. E. F. Rybaczewski, B. L. Neff, J. S. Waugh, and J. S. Sherfinski, High resolution ^{13}C NMR in solids: ^{13}C local fields of CH , CH_2 , and CH_3 , *J. Chem. Phys.* **67**, 1231–1236 (1977).
10. G. G. Webb and K. W. Zilm, Asynchronous MASSLF spectroscopy: A convenient method for assigning solid-state carbon-13 CPMAS spectra, *J. Am. Chem. Soc.* **111**, 2455–2463 (1989).
11. N. K. Sethi, Carbon-13 CP/MAS spectral assignment with one-dimensional separated-local-field spectroscopy, *J. Magn. Reson. A* **94**, 352–361 (1991).
12. X. Wu, S. T. Burns, and K. W. Zilm, Spectral editing in CPMAS NMR. Generating subspectra based on proton multiplicities, *J. Magn. Reson. A* **111**, 29–36 (1994).